

1 Run Title: Fine-scale nitrogen dynamics

2 **Title: Green light: gross primary production influences seasonal stream N export by**  
3 **controlling fine-scale N dynamics**

4 **Authors**

5 *Anna Lupon<sup>1</sup>, Eugènia Martí<sup>2</sup>, Francesc Sabater<sup>1</sup> Susana Bernal<sup>1,2</sup>*

6 **Affiliations**

7 <sup>1</sup>Department d'Ecologia, Facultat de Biologia, Universitat de Barcelona, Av. Diagonal 643,  
8 08028, Barcelona, Spain.

9 <sup>2</sup>Integrative Freshwater Ecology Group, Center for Advanced Studies of Blanes (CEAB-CSIC),  
10 Accés a la Cala Sant Francesc 14, 17300, Blanes, Girona, Spain.

11 **Corresponding author:** Anna Lupon. [alupon@ub.edu](mailto:alupon@ub.edu)

12

13 **Abstract:**

14 Monitoring nutrient concentrations at fine-scale temporal resolution contributes to a better  
15 understanding of nutrient cycling in stream ecosystems. However, the mechanisms underlying  
16 fine-scale nutrient dynamics and its implications for budget catchment fluxes are still poorly  
17 understood. To gain understanding on patterns and controls of fine-scale stream nitrogen (N)  
18 dynamics and to assess how they affect hydrological N fluxes, we explored diel variation in  
19 stream nitrate ( $\text{NO}_3^-$ ) concentration along a headwater stream with increasing riparian area and  
20 channel width. At the down-stream site, the highest day-night variations occurred in early-spring  
21 when stream  $\text{NO}_3^-$  concentrations were 13% higher at night than during day time. Such day-night  
22 variations were strongly related to daily light inputs ( $R^2=0.74$ ) and gross primary production  
23 (GPP) ( $R^2=0.74$ ), and they showed an excellent fit with day-night  $\text{NO}_3^-$  variations predicted from  
24 GPP ( $R^2=0.85$ ). These results suggest that diel fluctuations in stream  $\text{NO}_3^-$  concentration were  
25 mainly driven by photoautotrophic N uptake. Terrestrial influences were discarded because no  
26 simultaneous diel variations in stream discharge, riparian groundwater level, or riparian solute  
27 concentration were observed. In contrast to the down-stream site, no diel variations in  $\text{NO}_3^-$   
28 concentration occurred at the up-stream site likely because water temperature was colder (10 vs.  
29 12 °C) and light availability was lower (4 vs. 9  $\text{mol m}^{-2} \text{d}^{-1}$ ). Although daily GPP was between  
30 10-100 folds lower than daily respiration, photoautotrophic N uptake contributed to a 10%  
31 reduction in spring  $\text{NO}_3^-$  loads at the down-stream site. Our study clearly shows that the activity  
32 of photoautotrophs can substantially change over time and along the stream continuum in

33 response to key environmental drivers such as light and temperature, and further that its capacity  
34 to regulate diel and seasonal N fluxes can be important even in low productivity streams.

35 **Keywords**

36 Diel stream nitrate variation, photoautotrophic activity, in-stream nitrate uptake, stream  
37 metabolism, headwater forested streams.

38

39 **Introduction**

40 Human activity has doubled the availability of bioreactive nitrogen (N) worldwide, which  
41 compromises the function and biodiversity of terrestrial and freshwater ecosystems, as well as  
42 soil and water quality (Schlesinger 2009, Sutton et al. 2011). Nonetheless, biological activity can  
43 transform and retain a substantial amount of N inputs, and thus reduce the pervasive effects of  
44 excessive N in ecosystems (Bernhardt et al. 2002, Goodale et al. 2004). Within catchments,  
45 biogeochemical processes occurring at upland, riparian and aquatic ecosystems simultaneously  
46 contribute to N cycling and retention, and ultimately determine N export downstream (Bernhardt  
47 et al. 2005). In particular, there is a growing body of research demonstrating that streams and  
48 rivers have a high capacity to transform and retain N (Peterson et al. 2001, Tank et al. 2008),  
49 even though their ability to influence N export from catchments to downstream ecosystems is  
50 still under debate (Brookshire et al. 2009). This is mostly because water chemistry of stream and  
51 rivers integrates biogeochemical processes occurring at different spatial and temporal scales  
52 throughout the catchment, which complicates assessing the relative influence of in-stream and  
53 terrestrial processes on N exports (Sudduth et al. 2013). A better understanding of the  
54 mechanisms and drivers of N dynamics within fluvial ecosystems is critical to evaluate their  
55 capacity to modify N inputs from terrestrial sources.

56 Nitrate ( $\text{NO}_3^-$ ) is the predominant form of dissolved inorganic N (DIN) in fluvial ecosystems,  
57 and its uptake is mainly controlled by the metabolic activity of stream biota (Hall and Tank  
58 2003, Mulholland et al. 2008). Recently, monitoring at fine-scale temporal resolution in streams  
59 has provided examples of the close link between gross primary production and  $\text{NO}_3^-$  uptake (e.g.

60 Johnson et al. 2006, Roberts and Mulholland 2007, Heffernan and Cohen 2010). These studies  
61 have found an inverse relationship between fine-scale stream  $\text{NO}_3^-$  and dissolved oxygen (DO)  
62 concentrations, where lower  $\text{NO}_3^-$  and higher DO were observed during day- than night-time.  
63 This diel pattern of stream  $\text{NO}_3^-$  concentration has been mainly associated with photoautotrophic  
64 activity because the assimilation of  $\text{NO}_3^-$  by benthic algae needs light energy to reduce this form  
65 of DIN to ammonium (Huppe and Turpin 1994). However, diel  $\text{NO}_3^-$  patterns can also be driven  
66 by other processes such as diel fluctuations of riparian groundwater (Flewelling et al. 2013),  
67 diurnal in-stream nitrification (Gammons et al. 2011) and nocturnal in-stream denitrification  
68 (Baulch et al. 2012). Therefore, elucidating the potential mechanisms controlling diel variations  
69 in stream nutrient concentration remains a great challenge in stream ecology (Scholefield et al.  
70 2005, Pellerin et al. 2009). Moreover, the potential of fine-scale N dynamics to vary catchment N  
71 fluxes is still poorly understood because studies so far have been mainly performed during short  
72 time periods and within individual reaches.

73 The goal of this study was to investigate patterns and controls of diel variation in stream  $\text{NO}_3^-$   
74 concentration and to assess how these diel fluctuations influence N fluxes along a stream  
75 continuum with increasing riparian area and channel width. We hypothesized that stream  
76 metabolism will drive diel variations in stream  $\text{NO}_3^-$  concentration. We would expect a positive  
77 relationship between daily GPP and diel variations in stream  $\text{NO}_3^-$  concentration if  
78 photoautotrophic activity was the major control of fine-scale N dynamics. In this case, the largest  
79 diel  $\text{NO}_3^-$  variations would be observed during spring and at the downstream-most site, which is  
80 the widest and the most exposed to light. Conversely, if heterotrophic activity is the main control  
81 of fine-scale N dynamics, diel  $\text{NO}_3^-$  variations would be positively related to ecosystem

82 respiration (ER). Since stream water chemistry integrates processes occurring within the entire  
83 catchment, we also considered the alternative hypothesis that terrestrial or riparian processes will  
84 control fine-scale N patterns. In this case, we expected a positive relationship between diel  
85 variations in  $\text{NO}_3^-$  concentration in the stream and in riparian groundwater inputs, especially  
86 during the vegetative period when water and nutrient uptake by trees is the highest.

87 To evaluate these hypotheses, we measured diel variations in stream  $\text{NO}_3^-$  concentration together  
88 with stream metabolism, discharge, stream conservative tracer concentration (chloride), and  
89 riparian groundwater level and chemistry. Results from this study highlight the relevance of fine-  
90 scale temporal nutrient dynamics to understand the mechanisms underlying in-stream nutrient  
91 cycling, as well as to assess patterns of in-stream N removal and catchment nutrient fluxes at  
92 long-term scales.

## 93 **Materials and Methods**

### 94 *Study site*

95 The research was conducted at the Font del Regàs stream, which drains a 14.2 km<sup>2</sup> catchment in  
96 the Montseny Natural Park, NE Spain (41°50'N, 2°30'E, 500-1500 m a.s.l.). The catchment is  
97 dominated by biotitic granite (ICC 2010) and it is mainly covered by evergreen oak (*Quercus*  
98 *ilex*) and beech (*Fagus sylvatica*) forests. The climate of the area is typical sub-humid  
99 Mediterranean, with mild winters and warm summers. The meteorological station located at the  
100 study catchment recorded a mean annual precipitation of  $971.5 \pm 140.7$  mm (mean  $\pm$  SD) during  
101 the study period (2010-2012), which falls within the long-term mean for this region ( $924.7 \pm$

102 151.2 mm, period: 1940-2000). Similarly, mean annual temperature during the study period ( $13 \pm$   
103  $6 \text{ }^\circ\text{C}$ ) was close to the long-term mean ( $12.1 \pm 2.5 \text{ }^\circ\text{C}$ , period: 1940-2000).

104 We selected three sampling sites along 3 km of the Font del Regàs stream (Figure 1). The up-  
105 stream site (800 m a.s.l., 2.4 km from headwaters) was 1.7 m-wide stream with a poorly  
106 developed riparian forest composed of *Fagus sylvatica* and *Quercus ilex*. The mid-stream site  
107 (650 m a.s.l., 4.1 km from headwaters) was a 2.5 m-wide stream flanked by a mixed forest of  
108 typically riparian tree species such as *Alnus glutinosa* and *Fraxinus excelsior*. The down-stream  
109 site (500 m a.s.l., 5.3 km from headwaters) was the widest (wetted width = 3.1 m) and it had a  
110 well-developed riparian forest (~30 m wide) consisting mainly of *Robinea pseudoacacia*,  
111 *Populus nigra* and *A. glutinosa*.

112 The three sampling sites showed well-preserved channel morphology with a riffle-run structure.  
113 The streambed was mainly composed of rock (~30%), cobbles (~25%) and gravel (~15%) at the  
114 up- and mid-stream sites, whereas rock (~25%), cobbles (~30%) and sand (~30%) were the  
115 dominant substrates at the down-stream site. During the period of study, stream discharge (Q)  
116 averaged  $22.6 \pm 18.7 \text{ L/s}$  at the up-stream site, and increased to  $78.3 \pm 52.9$  and  $89.4 \pm 58.1 \text{ L/s}$   
117 at the mid- and down-stream sites, respectively, that were located downstream of the two main  
118 tributaries discharging to the mainstem (Figure 1). Stream DIN concentration averaged  $0.28 \pm$   
119  $0.09$ ,  $0.17 \pm 0.07$ , and  $0.19 \pm 0.08 \text{ mg N/L}$  at the up-, mid- and down-stream sites, respectively,  
120  $\text{NO}_3^-$  being the predominant form (> 85%). In all cases,  $\text{NH}_4^+$  concentration was low (<  $0.02 \text{ mg}$   
121  $\text{N L}^{-1}$ ) and it represented a small fraction (< 15%) of total DIN. Stream chloride ( $\text{Cl}^-$ )  
122 concentration increased along the stream continuum, from  $6.21 \pm 1.34 \text{ mg/L}$  at the up-stream site  
123 to  $8.06 \pm 1.02 \text{ mg/L}$  at the down-stream site. The riparian groundwater level (~ 2 m from the

124 stream channel) was  $0.5 \pm 0.1$  m below the soil surface (Bernal et al., 2015). At the down-stream  
125 site, mean riparian groundwater concentration was  $0.4 \pm 0.2$  mg N/L for  $\text{NO}_3^-$ ,  $11.4 \pm 4$  mg/L for  
126  $\text{Cl}^-$ , and  $4.2 \pm 1.5$  mg  $\text{O}_2$ /L for DO (averaged from 7 piezometers) (Poblador, unpublished data).

### 127 *Field sampling and laboratory analysis*

128 The field sampling was performed during two consecutive water years (2010-2011 and 2011-  
129 2012), each of which was devoted to accomplish different complementary objectives of our  
130 research. From September 2010 to August 2011 (water-year 2010-2011), we collected stream  
131 water samples twice a week at 12-hour intervals at the three sampling sites (up-, mid-, and down-  
132 stream) in order to explore the temporal pattern of diel variation in stream  $\text{NO}_3^-$  and  $\text{Cl}^-$   
133 concentrations along the study elevation gradient. We considered  $\text{Cl}^-$  as a conservative solute,  
134 little affected by biogeochemical processes (Kirchner et al. 2001). Moreover, we collected water  
135 samples every day (at noon) to calculate stream solute loads (see below). At each sampling site,  
136 water samples were collected with an auto-sampler (Teledyne Isco Model 1612), which was  
137 connected to a water pressure sensor (HOBO U20-001-04) that monitored stream water level at  
138 15-min intervals. Fortnightly, we measured Q at each sampling site by using the “slug” chloride  
139 addition method technique (Gordon et al. 1992). We inferred instantaneous Q from water level  
140 measurements by estimating the linear regression between stream water level and empirically  
141 measured Q (n = 57, 60 and 61 for up-, mid- and down-stream sites, respectively; in all cases:  $R^2$   
142 > 0.97).

143 From March to July 2012 (spring 2012), we focused on investigating the relationship between  
144 the diel variation in stream  $\text{NO}_3^-$  concentration and daily stream metabolism. The sampling effort



145 was concentrated at the down-stream site, where both stream metabolism and diel variations in  
146 stream  $\text{NO}_3^-$  concentration were expected to be the highest. A Teledyne Isco auto-sampler was  
147 used to collect stream water samples at 6-hour intervals: mid-night (0h), dawn (6h), noon (12h)  
148 and before sunset (18h). Instantaneous Q was measured as in 2010-2011. Daily stream  
149 metabolism was calculated from stream DO (in  $\text{mg O}_2 \text{ L}^{-1}$ ) recorded at 30-min intervals with an  
150 YSI ProODO oxymeter. We examined whether diel variations in stream solute concentration  
151 were related to riparian groundwater table fluctuations by monitoring riparian groundwater level  
152 (every 15 min),  $\text{NO}_3^-$  and  $\text{Cl}^-$  concentrations (every 12 hours) and DO concentration (every 30-  
153 min) at a piezometer placed  $\sim 2$  m from the stream channel. On average, riparian groundwater  
154 level and solute concentrations differed  $< 9\%$  between this piezometer and 6 others located  
155 nearby; and thus we considered this piezometer representative of riparian groundwater at the  
156 down-stream site (Poblador, unpublished data). In addition, we monitored the temporal pattern of  
157 temperature and light inputs to the stream along the study elevation gradient by installing HOBO  
158 sensors (HOBO U20-001-04) at the three sampling sites. The HOBOs recorded stream water  
159 temperature and photosynthetic active radiation (PAR) at 30-min intervals.

160 All water samples were filtered (Whatman GF/F) and kept cold ( $< 4$  °C) until laboratory analysis  
161 ( $< 24$ h after collection). Water samples were analyzed for  $\text{Cl}^-$  and for DIN ( $\text{NO}_3^-$  and  $\text{NH}_4^+$ ).  $\text{Cl}^-$   
162 was analyzed by ionic chromatography (Compact IC-761, Methrom).  $\text{NO}_3^-$  was analyzed by the  
163 cadmium reduction method (Keeney and Nelson 1982) using a Technicon Autoanalyzer  
164 (Technicon 1976).  $\text{NH}_4^+$  was manually analyzed by the salicylate-nitropruside method (Baethgen  
165 and Alley 1989) using a spectrophotometer (PharmaSpec UV-1700 SHIMADZU). Stream  $\text{NH}_4^+$

166 concentration was low and show no diel variation for any of the three stream sites, and thus  $\text{NH}_4^+$   
167 was not included in further data analysis.

### 168 *Data analysis*

169 *Temperature and light conditions.* We explored whether environmental conditions favoring in-  
170 stream photoautotrophic activity (temperature and PAR) were similar along the study stream  
171 continuum. For each sampling site, we calculated mean daily temperature (T, in °C) and  
172 accumulated daily PAR ( $\Sigma\text{PAR}$ , in  $\text{mol m}^{-2} \text{d}^{-1}$ ), and then we computed the number of days for  
173 which T and  $\Sigma\text{PAR}$  were optimal for photoautotrophic activity. Moreover, we computed the  
174 number of hours per day during which instantaneous PAR ( $\text{PAR}_i$ , in  $\mu\text{mol m}^{-2} \text{s}^{-1}$ ) was optimal  
175 for photosynthetic activity. We considered  $T = 10^\circ\text{C}$  as the threshold upon which  
176 photoautotrophs are not temperature limited (DeNicola 1996). A value of  $\Sigma\text{PAR} = 4 \text{ mol m}^{-2} \text{d}^{-1}$   
177 was considered the minimum daily input of light required to ensure the activity of  
178 photoautotrophs (Hill et al. 1995). Finally, we assumed that  $\text{PAR}_i > 200 \mu\text{mol m}^{-2} \text{s}^{-1}$  was the  
179 optimal irradiance for photosynthetic activity (Hill et al. 1995). Differences in T,  $\Sigma\text{PAR}$  and  
180  $\text{PAR}_i$  between the three sampling sites were established with a Wilcoxon paired rank sum test  
181 (Zar 2010).

182 *Temporal pattern of stream solute concentrations.* We examined the temporal pattern of day-  
183 night variations in  $\text{Cl}^-$  and  $\text{NO}_3^-$  concentrations by calculating the relative difference between  
184 midnight and noon solute concentrations ( $\Delta_{\text{solute}}$ , in %) with the following equation:

$$185 \quad \Delta_{\text{solute}} = \frac{[\text{solute}]_{0\text{h}} - [\text{solute}]_{12\text{h}}}{[\text{solute}]_{0\text{h}}} \times 100, \quad (1)$$

186 where  $[\text{solute}]_{0\text{h}}$  and  $[\text{solute}]_{12\text{h}}$  are the solute concentration (in mg/L) at midnight and noon,  
187 respectively. Values of  $\Delta_{\text{solute}} \sim 0$  indicate small or null variation in solute concentration between  
188 day and night, as expected for conservative solutes if the contribution of water sources to stream  
189 runoff does not vary between day and night time. Values of  $\Delta_{\text{solute}} > 0$  indicate higher solute  
190 concentrations at night than at day time, whereas values of  $\Delta_{\text{solute}} < 0$  indicate the opposite.  
191 Previous studies have shown that peaks of  $\text{NO}_3^-$  concentration often occur near predawn and  
192 minima later in the afternoon (Heffernan and Cohen 2010, Halliday et al. 2013). Therefore,  
193 values of  $\Delta_{\text{solute}}$  may underestimate, to some extent, the amplitude of diel variation because we  
194 collected the night-time sample at midnight.

195 To explore whether day-night variations in solute concentration were significant, we compared  
196 noon and midnight concentrations of either,  $\text{Cl}^-$  or  $\text{NO}_3^-$  by applying a Wilcoxon paired rank sum  
197 test. For the water year 2010-2011, we compared midnight and noon solute concentrations for  
198 each month and for each sampling site. For spring 2012, we compared midnight and noon solute  
199 concentrations at the down-stream site for each week for both stream and riparian groundwater.

200 To examine the potential influence of day-night variations in  $\text{NO}_3^-$  concentration on the 2010-  
201 2011 stream  $\text{NO}_3^-$  flux, we calculated the stream  $\text{NO}_3^-$  flux from the down-stream site with and  
202 without including day-night variations of  $\text{NO}_3^-$  concentration. The annual load of  $\text{NO}_3^-$  was  
203 calculated by multiplying instantaneous  $Q$  by stream  $\text{NO}_3^-$  concentration and integrating  
204 instantaneous  $\text{NO}_3^-$  loads over the water year (from 1 September to 31 August). To account for  
205 day-night variations, instantaneous stream  $\text{NO}_3^-$  concentration was estimated by linearly  
206 interpolating  $\text{NO}_3^-$  concentrations measured at noon and midnight, whereas only noon values of

207  $\text{NO}_3^-$  concentration were considered when excluding day-night variation. Because midnight  
208 samples were collected twice a week, instantaneous midnight stream  $\text{NO}_3^-$  concentration for each  
209 day was estimated by linearly interpolating midnight  $\text{NO}_3^-$  concentrations measured during  
210 consecutive sampling dates. Differences between the two approaches (with and without day-  
211 night  $\text{NO}_3^-$  concentration) were attributed to the effect of in-stream processes on stream  $\text{NO}_3^-$   
212 concentrations. The same procedure was repeated to calculate stream  $\text{NO}_3^-$  loads in spring 2012.

213 *Stream metabolism.* During spring 2012, we calculated daily rates of GPP and ER at the down-  
214 stream site by using the single-station diel DO change method (Bott 2006). This method was  
215 appropriate because in-stream conditions were uniform throughout the reach and groundwater  
216 inputs were small compared to stream discharge (<10%) (Bott 2006). DO curves were corrected  
217 for the reaeration flux by applying the night-time regression method to estimate the reaeration  
218 coefficient (Young and Huryn 1998). Daily ER was estimated by averaging the change in night  
219 time reaeration-corrected DO at 30 min interval and multiplying it by 24 hours, assuming that  
220 instantaneous ER was constant during the entire day (Bott 2006). Daily GPP was computed by  
221 integrating the difference between the change in reaeration-corrected DO and ER at 30-min  
222 intervals (both measures in  $\text{mg O}_2 \text{ L}^{-1} \text{ min}^{-1}$ ). We multiplied GPP and ER by the mean reach  
223 depth (in m) to obtain areal estimates (in  $\text{g O}_2 \text{ m}^{-2} \text{ d}^{-1}$ ). Mean reach depth was calculated weekly  
224 by averaging the water column depth measured at 20-cm intervals across 5 transects along a 40-  
225 m reach.

226 We examined the relationship between environmental variables (T and  $\Sigma\text{PAR}$ ), metabolic rates  
227 (daily ER and daily GPP) and daily  $\Delta\text{NO}_3^-$  using linear regression models. We further investigated  
228 the contribution of GPP to diel variations in stream  $\text{NO}_3^-$  concentration by comparing measured

229  $\text{NO}_3^-$  concentrations with those predicted based only on stoichiometric principles (Hall and Tank  
230 2003). First, we inferred instantaneous  $\text{NO}_3^-$  uptake rates by the stream photoautotrophic  
231 community ( $U_{\text{GPP}}$ ,  $\text{mg N L}^{-1} \text{ min}^{-1}$ ) from instantaneous GPP ( $\text{mg O}_2 \text{ L}^{-1} \text{ min}^{-1}$ ). We assumed that  
232 (i) the molar ratio for  $\text{CO}_2:\text{O}_2$  was 1:1 during photosynthesis (Hall and Tank 2003), and (ii) the  
233 C:N ratio of the epilithic photoautotrophic community was 14:1 (C:N =  $13.7 \pm 1.3$  in light  
234 exposed epilithic biofilm at the study stream, Pastor et al. 2014). We acknowledge that these are  
235 rough estimates because not all GPP is translated into biomass accrual (Hall and Beaulieu 2013),  
236 and not all epilithic biofilm is composed of photoautotrophic organisms (Volkmar et al. 2011).  
237 However, this was a useful exercise for our purposes because we inferred N uptake by  
238 photoautotrophs from stoichiometric principles, independently of diel variations in stream  $\text{NO}_3^-$   
239 concentration. Then, at each time step ( $t = 0, 6, 12,$  and  $18\text{h}$ ), we calculated the predicted stream  
240  $\text{NO}_3^-$  concentration ( $[\text{NO}_3]'_t$ , in  $\text{mg N/L}$ ) as follows:

$$241 \quad [\text{NO}_3]'_t = [\text{NO}_3]'_{t-1} - (\overline{U_{\text{GPP}}} \times \Delta t) \quad (2)$$

242 where  $[\text{NO}_3]'_{t-1}$  is the predicted stream  $\text{NO}_3^-$  concentration (in  $\text{mg N L}^{-1}$ ) at sampling time  $t-1$ ,  
243  $\overline{U_{\text{GPP}}}$  is the average  $U_{\text{GPP}}$  between sampling time intervals, and  $\Delta t$  is the time interval between  
244 sampling times (360 min) (Heffernan and Cohen 2010). The initial condition to run the model  
245 was considered to be the observed stream  $\text{NO}_3^-$  concentration at the beginning of spring 2012.  
246 We evaluated the goodness of fit between predicted and observed  $\text{NO}_3^-$  concentration and  $\Delta_{\text{NO}_3}$   
247 by ordinary least squares. Moreover, we tested whether the slope of the linear regression between  
248 predicted and observed values was similar to 1 with a slope test (Zar 2010). We expected a slope  
249 similar to 1 between predicted and observed values if GPP is the main driver of diel variations in

250 stream  $\text{NO}_3^-$  concentration. Further, the residuals between predicted and observed  $\Delta_{\text{NO}_3}$  were  
251 examined for evaluating the ability of the model to predict changes in  $\Delta_{\text{NO}_3}$  over time.

252 All the statistical analyses were carried out with the R 2.15.1 statistical software (R-project  
253 2008). We chose non-parametric tests for the statistical analysis because not all data sets had a  
254 normal distribution. In all cases, differences were considered statistically significant when  $p <$   
255 0.05.

## 256 **Results**

### 257 *Temperature and light inputs along the stream*

258 During spring 2012, environmental conditions were more favorable for photosynthetic activity at  
259 the mid- and down-stream sites than at the up-stream site. Both T and  $\Sigma\text{PAR}$  were higher at the  
260 down- than at the up-stream site (Table 1). Moreover,  $T > 10^\circ\text{C}$  was reached during 50%, 85%,  
261 and 90% of the days at the up-, mid-, and down-stream sites, respectively (Table 1, Figure 2a).

262 The percentage of days with  $\Sigma\text{PAR} > 4 \text{ mol m}^{-2} \text{ d}^{-1}$  increased along the stream continuum, being  
263 59%, 74% and 93% at the up-, mid-, and down-stream sites, respectively (Table 1, Figure 2b).

264 At the down-stream site, T remained around  $9.6 \pm 2.1^\circ\text{C}$  from mid-March to mid-April, and then  
265 it increased to  $15^\circ\text{C}$  until the end of the study period in July (Figure 3a). Diel variations in  
266 temperature remained small during spring 2012, being  $1.5 \pm 0.8^\circ\text{C}$  higher at noon than at night-  
267 time (Figure 3a). Light inputs to the stream ( $\text{PAR}_i$ ) increased from mid-March until two weeks  
268 after the riparian leaf-out in early-April (Figure 3b). As the riparian canopy developed (from

269 mid-April to late-May),  $PAR_i$  and diel variation in  $PAR_i$  sharply decreased, and then remained  
270 low until the end of the experiment in July (Figure 3b).

271 *Temporal patterns of day-night variation in stream and riparian groundwater solute*  
272 *concentrations*

273 During the water year 2010-2011,  $Cl^-$  concentration did not differ between midnight and noon in  
274 any month and at any of the three stream sites (for the 12 months and the 3 sites: Wilcoxon  
275 paired rank sum test,  $Z > Z_{0.05}$ ,  $df = 11$ ,  $p > 0.05$ ) (Figure 4, white circles). In contrast, the day-  
276 night variation in  $NO_3^-$  concentration differed between stream sites. At the up-stream site, there  
277 were no differences between midnight and noon stream  $NO_3^-$  concentrations in any month (for  
278 the 12 months:  $Z > Z_{0.05}$ ,  $df = 11$ ,  $p > 0.05$ ) (Figure 4a, black circles). At the mid- and down-  
279 stream sites, stream  $NO_3^-$  concentrations at midnight were higher than at noon during spring  
280 months (from April to June, and from April to May for the mid- and down-stream sites,  
281 respectively; in all cases  $Z < Z_{0.05}$ ,  $df = 11$ ,  $p < 0.05$ ). During this period, monthly median  $\Delta_{NO_3}$   
282 ranged from 6.3 to 19.1% (Figure 4b and 4c, black circles). In November, stream  $NO_3^-$   
283 concentrations were 12.8% higher at noon than at midnight at the down-stream site ( $Z = -1.825$ ,  
284  $df = 11$ ,  $p < 0.05$ ) (Figure 4c, black circles).

285 Such day-night variations in stream  $NO_3^-$  concentration influenced stream N fluxes mainly  
286 during spring, reducing the  $NO_3^-$  load at the down-stream site by 11%. The reduction in stream  
287  $NO_3^-$  load was similar during spring 2012 (9%). During autumn, winter and summer, diel  
288 variations in  $NO_3^-$  concentration had a small effect on stream  $NO_3^-$  loads (< 5%).

289 During spring 2012, the diel pattern of stream solute concentrations at the down-stream site was  
290 similar to spring 2011. Stream  $\text{Cl}^-$  concentration averaged  $8.3 \pm 0.3$  mg/L and it slightly  
291 increased from March to July, showing the opposite pattern than stream Q (Figure 3c and Figure  
292 3d). Diel variations for both Q and  $\text{Cl}^-$  concentration remained low ( $< 5\%$ ) and did not differ  
293 between midnight and noon throughout the sampling period (from March to June:  $Z > Z_{0.05}$ ,  $df =$   
294  $6$ ,  $p > 0.1$ ) (Figure 5a, white circles). Stream  $\text{NO}_3^-$  concentration ranged from 0.12 to 0.23 mg  
295 N/L, and showed higher values at midnight than at noon from mid-March to late-May (for each  
296 of the 12 weeks:  $Z < Z_{0.05}$ ,  $df = 6$ ,  $p < 0.05$ ) (Figure 3e). The  $\Delta_{\text{NO}_3}$  increased from mid-March to  
297 the beginning of May (three weeks after the riparian leaf-out), and then declined until the  
298 riparian canopy was fully closed in June (Figure 5a, black circles). No day-night variations in  
299 stream  $\text{NO}_3^-$  concentration were found later on (for all June weeks:  $Z > Z_{0.05,6}$ ,  $df = 6$ ,  $p > 0.1$ ).

300 During spring 2012, riparian groundwater DO concentration averaged  $4.72 \pm 1.47$  mg  $\text{O}_2$ /L and  
301 it slightly decreased from March to June, showing the same pattern than riparian groundwater  
302 level. Riparian groundwater concentration averaged  $11.3 \pm 0.5$  mg/L for  $\text{Cl}^-$  and  $0.46 \pm 0.08$  mg  
303 N/L for  $\text{NO}_3^-$ . Diel variations in riparian groundwater level, DO,  $\text{Cl}^-$  and  $\text{NO}_3^-$  concentration did  
304 not differ between midnight and noon throughout the sampling period (for the four variables and  
305 for each of the 15 weeks:  $Z > Z_{0.05}$ ,  $df = 6$ ,  $p > 0.1$ ) (Figure 5b).

### 306 *Relationship between diel variation in nitrate concentration and stream metabolism*

307 During spring 2012, daily rates of ER at the down-stream site ranged from 5.5 to 10.0 g  $\text{O}_2$   $\text{m}^{-2}$   $\text{d}^{-1}$   
308  $^1$ , increasing from April to mid-May and then remaining relatively constant at  $8.4 \pm 1.0$  g  $\text{O}_2$   $\text{m}^{-2}$   
309  $\text{d}^{-1}$  (Figure 2c). This temporal pattern was positively related to the temporal pattern of T (linear



310 regression [l.r.],  $R^2 = 0.38$ ,  $p < 0.05$ ,  $n = 44$ ). Daily rates of GPP were between 10-100 fold lower  
311 than daily rates of ER, indicating that stream metabolism was dominated by heterotrophic  
312 activity during spring. Daily rates of GPP increased from April ( $0.35 \text{ g O}_2 \text{ m}^{-2} \text{ d}^{-1}$ ) to mid-May  
313 ( $0.64 \text{ g O}_2 \text{ m}^{-2} \text{ d}^{-1}$ ), and then decreased until June ( $0.07 \text{ g O}_2 \text{ m}^{-2} \text{ d}^{-1}$ ) (Figure 2c). This temporal  
314 pattern was positively related to the temporal pattern of  $\Sigma\text{PAR}$  (Figure 6a). No relationship was  
315 found between daily rates of GPP and ER (l.r.,  $R^2 = 0.02$ ,  $p > 0.1$ ,  $n = 44$ ).

316 There was no relationship between daily  $\Delta\text{NO}_3$  and daily ER (l.r.,  $R^2 = 0.01$ ,  $p > 0.1$ ,  $n = 44$ ),  
317 while daily  $\Delta\text{NO}_3$  was positively related to daily GPP (Figure 6b). There was a good fit between  
318 observed stream  $\text{NO}_3^-$  concentrations and those predicted from stoichiometric principles as  
319 indicated by both the strong relationship between observed and predicted values (l.r.,  $R^2 = 0.73$ ,  $p$   
320  $< 0.001$ ,  $n = 201$ ), and non-significant divergences from the 1:1 line (slope test,  $F = 1.01$ ,  $df =$   
321  $200$ ,  $p > 0.1$ ). Similarly, there was a good fit between observed and predicted  $\Delta\text{NO}_3$  (l.r.,  $R^2 =$   
322  $0.85$ ,  $p < 0.001$ ,  $n = 44$ ; slope test,  $F = 0.55$ ,  $df = 43$ ,  $p > 0.1$ ) (Figure 6c). Divergences between  
323 observed and predicted  $\Delta\text{NO}_3$  were  $< 4\%$  during March, April and May, while on average  
324 predicted values were overestimated by  $14\%$  in June.

## 325 **Discussion**

326 This study aimed to investigate the importance of terrestrial and in-stream biogeochemical  
327 processes on controlling fine-scale temporal N dynamics along a stream continuum, and to assess  
328 the influence of such diel  $\text{NO}_3^-$  fluctuations on stream N fluxes at seasonal scale. Our results  
329 indicated that the temporal pattern of diel variation in stream  $\text{NO}_3^-$  concentration varied  
330 substantially along the stream. No diel  $\text{NO}_3^-$  variations were observed at the up-stream site, while

331 day-night variations in  $\text{NO}_3^-$  concentration peaked during the onset of riparian leaf emergence at  
332 the mid- and down-stream sites as reported in previous studies (Roberts and Mulholland 2007,  
333 Rusjan and Mikoš 2009). These contrasting patterns in fine-scale N dynamics were accompanied  
334 by longitudinal increases in temperature and light availability, suggesting that these two  
335 environmental factors were controlling the extent to which in-stream processes modified fine-  
336 scale  $\text{NO}_3^-$  dynamics along the stream continuum.

337 The results obtained during spring 2012 convincingly showed that terrestrial processes did not  
338 control diel variations in  $\text{NO}_3^-$  concentration because no simultaneous diel variations in stream  
339 discharge, riparian groundwater level or N concentration were observed. Moreover, simple mass  
340 balance calculations indicate that hydrological mixing with riparian groundwater inputs could  
341 not explain midnight increases in stream  $\text{NO}_3^-$  concentration because median  $\Delta_{\text{NO}_3}$  would then  
342 have been 0.6% instead of 13% (Appendix A). Conversely, the strong relationship and  
343 synchronicity between daily GPP and  $\Delta_{\text{NO}_3}$  supports the hypothesis that in-stream  
344 photoautotrophic activity was a major driver of the observed diel variations in stream  $\text{NO}_3^-$   
345 concentration. These results are in agreement with findings from lowland rivers (Heffernan and  
346 Cohen 2010), headwater forested streams (Roberts and Mulholland 2007), and even coastal  
347 ecosystems (Johnson et al. 2006). Yet, these previous studies were performed during periods of  
348 relatively high photoautotrophic activity ( $\text{GPP} = 5\text{-}20 \text{ g O}_2 \text{ m}^{-2} \text{ d}^{-1}$ ,  $\text{GPP:ER} \sim 1$ ) compared to the  
349 values measured in this study ( $\text{GPP} < 0.7 \text{ g O}_2 \text{ m}^{-2} \text{ d}^{-1}$ ,  $\text{GPP:ER} < 0.01$ ). Therefore, our study is  
350 novel in showing the potential of photoautotrophic activity to regulate in-stream  $\text{NO}_3^-$  dynamics  
351 even in extremely low productivity streams dominated by heterotrophic metabolism.

352 Our results add to the growing body of research demonstrating that GPP is a strong driver of in-  
353 stream  $\text{NO}_3^-$  uptake (Hall and Tank 2003, Mulholland et al. 2008), though the relationship  
354 between stream metabolism and fine-scale N dynamics can vary among streams. For instance,  
355 diel  $\text{NO}_3^-$  variations in April were similar (10-20  $\mu\text{g N/L}$ ) between Walker Branch (TN, USA;  
356 Roberts and Mulholland 2007) and Font del Regàs (this study), despite daily rates of GPP that  
357 were 10 fold larger at Walker Branch. On the other hand, GPP at Walker Branch was similar to  
358 Sycamore Creek (AZ, USA; Grimm 1987) and Ichetucknee river (FL, USA; Heffernan and  
359 Cohen 2010) (7-14  $\text{g O}_2 \text{ m}^{-2} \text{ d}^{-1}$ ), though diel  $\text{NO}_3^-$  variations were 4-6 fold lower at Walker  
360 Branch (10-20 vs. 75-100  $\mu\text{g N/L}$ ). Midday decline in stream  $\text{NO}_3^-$  concentrations is likely driven  
361 by photoautotrophic N demand relative to N supply (Sterner and Elser 2002, Appling and  
362 Heffernan 2014). Thus, divergences between GPP and diel  $\text{NO}_3^-$  variations among streams could  
363 be explained by differences in both N availability (from 0.12 to 0.42  $\text{mg N/L}$  at Font del Regàs  
364 and Ichetucknee river, respectively) and the C:N ratio of primary uptake compartments (from  
365 14:1 in Font del Regàs epilithic biofilms to 25:1 in Ichetucknee macrophytes). A good  
366 assessment of the stream biota stoichiometry is thus crucial to constrain the uncertainty  
367 associated with mechanistic models linking stream metabolism and fine-scale nutrient dynamics.

368 Despite the strong match between day-night variations measured at the down-stream site and  
369 those predicted from GPP instantaneous rates during early spring, divergences between measured  
370 and predicted  $\Delta_{\text{NO}_3}$  were evident in late spring. These biases in model prediction could be  
371 explained by changes in the stoichiometry of the algal community (Sterner and Elser 2002,  
372 Heffernan and Cohen 2010) or in the respiration rate of photoautotrophs (Hall and Beaulieu  
373 2013), which could be induced by decreased light inputs after riparian leaf-out. Additionally,

374 these mismatches could be explained by shifts in the main processes regulating diel  $\text{NO}_3^-$   
375 variations after leaf-out such as in-stream nitrification or denitrification (Gammons et al. 2011,  
376 Baulch et al. 2012). Diel cycles of these two processes could probably be suited for day-night  
377  $\text{NO}_3^-$  variations during the peak of leaf litter accumulation in November, which resulted in  
378 midnight decline in stream  $\text{NO}_3^-$  concentrations (Laursen and Seitzinger 2004). However, it  
379 seems unlikely that nitrification could account for the observed diel  $\text{NO}_3^-$  patterns in spring  
380 because no diel variations in  $\text{NH}_4^+$  concentration occurred to support nitrification, while  
381 relatively high DO concentrations in the stream ( $10.7 \pm 0.5 \text{ mg O}_2/\text{L}$ ) and hyporheic zone ( $7.8 \pm$   
382  $1.6 \text{ mg O}_2/\text{L}$ ; Poblador, unpublished data) suggest low denitrification in stream sediments (Kemp  
383 and Dodds 2002, Johnson and Tank 2009). The lack of correlation between  $\Delta_{\text{NO}_3}$  and ER, further  
384 support that GPP was a major player regulating fine-scale  $\text{NO}_3^-$  dynamics. The current  
385 understanding of the influence of metabolism on stream N dynamics has been mostly based on  
386 correlational analysis (e.g. Hall and Tank 2003). Nonetheless, our study shows that  
387 stoichiometric models based on diel nutrient variation are complementary and powerful tools that  
388 can contribute to disentangle the mechanisms driving stream nutrient cycling over time and  
389 space.

390 There is still little research available on whether diel variations in nutrient concentration can  
391 have any implication at larger spatial and temporal scales, and how the mechanisms underlying  
392 such fine-scale patterns can ultimately modify catchment nutrient fluxes. Our study indicated  
393 that the contribution of photoautotrophic N uptake to regulate  $\text{NO}_3^-$  fluxes at the down-stream  
394 site was small in annual terms (4%), as expected for a low productivity stream such as Font del  
395 Regàs (Valett et al. 2008, Battin et al. 2008). However, during spring, increased

396 photoautotrophic N uptake led to a decrease in catchment  $\text{NO}_3^-$  export of  $\sim 20$  g N/ha, which was  
397 equivalent to a  $\sim 10\%$  reduction in the stream  $\text{NO}_3^-$  export. Since maxima  $\text{NO}_3^-$  and minima DO  
398 concentrations usually coincide over a daily cycle (Heffernan and Cohen 2010, Halliday et al.  
399 2013), our estimates may be slightly underestimated because we measured  $\text{NO}_3^-$  at 0h, while  
400 minima DO occurred between 0-3h. Nevertheless, we estimated a similar decrease in spring  
401  $\text{NO}_3^-$  loads (15 g N/ha,  $\sim 12\%$ ) for Walker Branch (38.4 ha, 6-14 L/s) based on mean  $\text{NO}_3^-$   
402 concentration (0.2-0.5 mg N/L) and  $\Delta_{\text{NO}_3}$  (2-15  $\mu\text{g}$  N/L) reported by Roberts and Mulholland  
403 (2007). These estimations for Font del Regàs and Walker Branch suggest that benthic algae are  
404 an important transitory sink of DIN in these headwater forested streams, similarly to the vernal  
405 dam described for spring ephemeral plants by Muller and Bormann (1976). Nonetheless, the  
406 relevance of photoautotrophic N retention at longer time scales will ultimately depend on the  
407 turnover rates of the primary uptake compartments, which can vary widely between epilithic  
408 biofilms (few days) to macrophytes (months) (Riis et al. 2012).

409 The influence of fine-scale N patterns on N fluxes could be even higher in open-canopy and  
410 lowland streams for which reported diel  $\text{NO}_3^-$  variations are larger than for headwater forested  
411 streams (Grimm 1987, Heffernan et al. 2010, Halliday et al. 2013). For instance, we estimated  
412 that spring diel  $\text{NO}_3^-$  variation may reduce catchment  $\text{NO}_3^-$  exports by  $\sim 70$  g N  $\text{ha}^{-1}$  ( $\sim 16\%$ ) at the  
413 Ichetucknee river (770  $\text{km}^2$ , 8900 L/s), based on mean daily minima and maxima  $\text{NO}_3^-$   
414 concentrations (0.38 and 0.46 mg N/L) reported by Hefferman and Cohen (2010). The  
415 contribution of fine-scale N dynamics to reduce catchment N export was even larger at the Upper  
416 Hafren river in UK (122 ha, 60 L/s), an open stream where spring diel  $\text{NO}_3^-$  variations (from  
417 0.014 to 0.018 mg N/L) reduced stream  $\text{NO}_3^-$  loads by 154 g N/ha (22 %) (Halliday et al. 2013).

418 These back-of-the-envelope calculations highlight that fine-scale N dynamics can not only  
419 indicate the preferential mechanisms of in-stream N uptake, but also provide a relevant  
420 evaluation of their contribution on regulating  $\text{NO}_3^-$  downstream fluxes at the catchment scale.

## 421 **Conclusions**

422 This study adds to the growing evidence demonstrating that in-stream processes can substantially  
423 modify stream N concentration and fluxes (Peterson et al. 2001, Bernhardt et al. 2005, Arango et  
424 al. 2008, Bernal et al. 2012). In-stream GPP was the major driver of diel variations in stream  
425  $\text{NO}_3^-$  concentration in this highly heterotrophic headwater stream, while the contribution of other  
426 in-stream, riparian, and upland processes was minimal. From a network perspective, the temporal  
427 pattern of such diel  $\text{NO}_3^-$  variations, and thus their influence on stream N fluxes, varied along the  
428 stream continuum depending on light and temperature regimes. Finally, and in line with previous  
429 work, our study indicates that discrete measurements performed at midday can limit our  
430 understanding of in-stream nutrient cycling as well as the assessment of reliable nutrient budgets  
431 at long time scales even in low productivity streams (Mulholland et al. 2006). These biases could  
432 be even larger (up to 15-20%) for highly productive streams given that the capacity of stream  
433 biota to regulate diel and seasonal stream N dynamics could increase along the river continuum,  
434 as observed in this study. Overall, monitoring of nutrient data at fine-scale temporal resolution  
435 can provide mechanistic explanations about the relevance of in-stream and terrestrial processes  
436 on regulating stream nutrient concentrations and their implications on long-term fluxes at the  
437 catchment scale.

438 **Acknowledgements**

439 We are thankful to Miquel Ribot and Sílvia Poblador for their invaluable assistance in the field,  
440 and to S. Poblador for providing data on Font del Regàs riparian groundwater and hyporheic  
441 zone . Special thanks are extended to Jennifer Drummond, Stuart Findlay and two anonymous  
442 reviewers for helpful comments on an earlier version of the manuscript. Financial supported was  
443 provided by the Spanish Government through the projects MONTES-Consolider (CSD2008-  
444 00040-MONTES) and MEDFORESTREAM (CGL2011-30590). AL was supported by a FPU  
445 PhD fellowship from the Spanish Ministry of Education and Science (AP-2009-3711). SB work  
446 was funded by the Spanish Research Council (JAE-DOC027), the Spanish CICT (Juan de la  
447 Cierva contract JCI-2008-177), European Social Funds (FSE), and the MEDFORESTREAM and  
448 NICUS (CGL-2014-55234-JIN) projects. We also thank site cooperators, including Vichy  
449 Catalan and the Catalan Water Agency (ACA) for permission to sample at the Font del Regàs  
450 catchment.

451 **References**

452 Appling, A. P., and J. B. Heffernan. 2014. Limitation and physiology mediate the fine-scale  
453 (de)coupling of biogeochemical cycles. *The American Naturalist* 184:384-406.

454 Baethgen, W., and M. Alley. 1989. A manual colorimetric procedure for ammonium nitrogen in  
455 soil and plant Kjeldahl digests. *Communications in Soil Science and Plant Analysis* 20:961–969.

456 Battin, T. J., L. A. Kaplan, S. Findlay, C. S. Hopkinson, E. Martí, A. I. Packman, J. D. Newbold,  
457 and F. Sabater. 2008. Biophysical controls on organic carbon fluxes in fluvial networks. *Nature*  
458 *Geoscience* 1:95–100.

459 Baulch, H. M., P. J. Dillon, R. Maranger, J. J. Venkiteswaran, H. F. Wilson, and S. L. Schiff.  
460 2012. Night and day: short-term variation in nitrogen chemistry and nitrous oxide emissions  
461 from streams. *Freshwater Biology* 57:509–525.

462 Bernal, S., A. Lupon, M. Ribot, F. Sabater, and E. Martí. 2015. Riparian and in-stream controls  
463 on nutrient concentrations along a headwater forested stream. *Biogeosciences* 12:1941-1954.

464 Bernhardt, E. S., R. O. Hall Jr., and G. E. Likens. 2002. Whole-system estimates of nitrification  
465 and nitrate uptake in streams of the Hubbard Brook experimental forest. *Ecosystems* 5:419–430.

466 Bernhardt, E. S., G. E. Likens, R. O. H. Jr, D. O. N. C. Buso, S. G. Fisher, T. M. Burton, J. L.  
467 Meyer, W. H. McDowell, M. S. Mayer, W. B. Bowden, S. E. G. Findlay, K. H. Macneale, R. S.  
468 Stelzer, and W. H. Lowe. 2005. Can't see the forest for the stream? In-stream processing and  
469 terrestrial nitrogen exports. *BioScience* 55:219–230.

470 Bott, T. L. 2006. Primary productivity and community respiration. *Pages 663–690 in* F. R. Hauer  
471 and G. A. Lamberti, *editors*. *Methods in stream ecology*. *Academic Press, San Diego, CA*.

472 Brookshire, J. E. N., H. M. Valett, and S. Gerber. 2009. Maintenance of terrestrial nutrient loss  
473 signatures during in-stream transport. *Ecology* 90:293–299.



474 DeNicola, D. M. 1996. Periphyton responses to temperature at different ecological levels. *Pages*  
475 *149–181 in* R. J. Stevenson, M. L. Bothwell, and R. L. Lowe, *editors*. *Algal Ecology*. Elsevier,  
476 *San Diego, CA*.

477 Flewelling, S. A., G. M. Hornberger, J. S. Herman, A. L. Mills, and W. M. Robertson. 2013. Diel  
478 patterns in coastal-stream nitrate concentrations linked to evapotranspiration in the riparian zone  
479 of a low-relief, agricultural catchment. *Hydrological Processes* 28:2150–2158.

480 Gammons, C. H., J. N. Babcock, S. R. Parker, and S. R. Poulson. 2011. Diel cycling and stable  
481 isotopes of dissolved oxygen, dissolved inorganic carbon, and nitrogenous species in a stream  
482 receiving treated municipal sewage. *Chemical Geology* 283:44–55.

483 Goodale, C. L., K. Lajtha, K. J. Nadelhoffer, E. W. Boyer, and N. A. Jaworski. 2004. Forest  
484 nitrogen sinks in large eastern U. S. watersheds : estimates from forest inventory and an  
485 ecosystem. *Biogeochemistry* 57/58:239–266.

486 Gordon, N. D., T. A. McMahon, B. L. Finlayson, C. J. Gippel, and R. J. Nathan. 1992. *Stream*  
487 *Hydrology: an introduction for Ecologists*. Pages 123 *in* J. Winley & Sons, *editors*. *Princeton-*  
488 *Hall, New Jersey, NJ*.

489 Grimm, N. B. 1987. Nitrogen dynamics during succession in a desert stream. *Ecology* 68:1157–  
490 1170.

491 Hall, R. O., and J. L. Tank. 2003. Ecosystem metabolism controls nitrogen uptake in streams in  
492 Grand Teton National Park, Wyoming. *Limnology and Oceanography* 48:1120–1128.

493 Hall, R. O., and J.J. Beaulieu. 2013. Estimating autotrophic respiration in streams using daily  
494 metabolism data. *Freshwater Science* 32: 507-516.

495 Halliday, S. J., R. A. Skeffington, A. J. Wade, C. Neal, B. Reynolds, D. Norris, and J. W.  
496 Kirchner. 2013. Upland streamwater nitrate dynamics across decadal to sub-daily timescales: a  
497 case study of Plynlimon, Wales. *Biogeosciences* 10:8013–8038.

498 Heffernan, J. B., and M. J. Cohen. 2010. Direct and indirect coupling of primary production and  
499 diel nitrate dynamics in a subtropical spring-fed river. *Limnology and Oceanography* 55:677–  
500 688.

501 Hill, W. R., P. J. Mulholland, and E. R. Marzolf. 2001. Stream ecosystem responses to forest leaf  
502 emergence in spring. *Ecology* 82:2306–2319.

503 Hill, W. R., M. G. Ryon, and E. M. Schilling. 1995. Light limitation in a stream ecosystem:  
504 responses by primary producers and consumers. *Ecology* 76:1297–1309.

505 Huppe, H. C., and D. H. Turpin. 1994. Integration of carbon and nitrogen-metabolism in plant  
506 and algal cells. *Annual Review of Plant Physiology and Plant Molecular Biology* 45:577–607.

507 Johnson, K. S., L. J. Coletti, and F. P. Chavez. 2006. Diel nitrate cycles observed with in situ  
508 sensors predict monthly and annual new production. *Deep Sea Research Part I: Oceanographic*  
509 *Research Papers* 53:561–573.

510 Johnson, L. T., and J. L. Tank. 2009. Diurnal variations in dissolved organic matter and  
511 ammonium uptake in six open-canopy streams. *Journal of the North American Benthological*  
512 *Society* 28:694–708.

513 Keeney, D. R., and D. W. Nelson. 1982. Nitrogen-inorganic forms. Pages 643–698 in A. L.  
514 Page, editor. *Methods of soil analysis. Part 2. Agronomy Monograph*. ASA and SSSA,  
515 Madison, WI.

516 Kemp, M. J., and W. K. Dodds. 2002. The influence of ammonium, nitrate, and dissolved  
517 oxygen concentrations on uptake, nitrification, and denitrification rates associated with prairie  
518 stream substrata. *Limnology and Oceanography* 47:1380–1393.

519 Kirchner, J. W., X. H. Feng, and C. Neal. 2001. Catchment-scale advection and dispersion as a  
520 mechanism for fractal scaling in stream tracer concentrations. *Journal of Hydrology* 254:82–101.

521 Laursen, A. E., and S. P. Seitzinger. 2004. Diurnal patterns of denitrification, oxygen  
522 consumption and nitrous oxide production in rivers measured at the whole-reach scale.  
523 *Freshwater Biology* 49:1448–1458.

524 Mulholland, P. J., S. A. Thomas, H. M. Valett, J. R. Webster, and J. Beaulieu. 2006. Effects of  
525 light on  $\text{NO}_3^-$  uptake in small forested streams: diurnal and day-to-day variations. *Journal of the*  
526 *North American Benthological Society* 25:583–595.

527 Mulholland, P. J., A. M. Helton, G. C. Poole, R. O. Hall Jr, S. K. Hamilton, B. J. Peterson, J. L.  
528 Tank, L. R. Ashkenas, L. W. Cooper, C. N. Dahm, W. K. Dodds, S. E. G. Findlay, S. V.  
529 Gregory, N. B. Grimm, S. L. Johnson, W. H. McDowell, J. L. Meyer, H. M. Valett, J. R.  
530 Webster, C. P. Arango, J. J. Beaulieu. M. J. Bernot, A. J. Burgin, C. L. Crenshaw, L. T. Johnson,  
531 B. R. Niederlehner, J. M. O'Brien, J. D. Potter, R. W. Sheibley, D. J. Sobota, and S. M. Thomas.

532 2008. Stream denitrification across biomes and its response to anthropogenic nitrate loading.  
533 *Nature* 452:202-206.

534 Muller, R. N., and F. H. Bormann. 1976. Role of *Erythronium americanum* Ker. on energy-flow  
535 and nutrient dynamics of a northern hardwood forest ecosystem. *Science* 193:1126–1128.

536 Pastor, A., J. L. Riera, M. Peipoch, L. Cañas, M.I Ribot, E. Gacia, E. Martí, and F. Sabater. 2014.  
537 Temporal variability of nitrogen stable isotopes in primary uptake compartments in four streams  
538 differing in human impacts. *Environmental Science and Technology* 48:6612–6619.

539 Pellerin, B. A., B. D. Downing, C. Kendall, R. A. Dahlgren, T. E. C. Kraus, J. Saraceno, R. G.  
540 M. Spencer, and B. A. Bergamaschi. 2009. Assessing the sources and magnitude of diurnal  
541 nitrate variability in the San Joaquin River (California) with an in situ optical nitrate sensor and  
542 dual nitrate isotopes. *Freshwater Biology* 54:376–387.

543 Peterson, B. J., W. M. Wollheim, P. J. Mulholland, J. R. Webster, J. L. Meyer, J. L. Tank, E.  
544 Martí, W. B. Bowden, H. M. Valett, A. E. Hershey, W. H. McDowell, W. K. Dodds, S. K.  
545 Hamilton, S. Gregory, and D. D. Morrall. 2001. Control of nitrogen export from watersheds by  
546 headwater streams. *Science* 292:86–90.

547 R Core Team. 2012. R: A language and environment for statistical computing. R Foundation for  
548 Statistical Computing, editors. Vienna, Austria.

549 Riis, T., W. K. Dodds, P. B. Kristensen, and A. J. Baisner. 2012. Nitrogen cycling and dynamics  
550 in a macrophyte-rich stream as determined by a  $^{15}\text{N-NH}_4^+$  release. *Freshwater Biology* 57: 1579–  
551 1591.

552 Roberts, B. J., and P. J. Mulholland. 2007. In-stream biotic control on nutrient biogeochemistry  
553 in a forested stream, West Fork of Walker Branch. *Journal of Geophysical Research*  
554 112:G04002.

555 Rusjan, S., and M. Mikoš. 2009. Seasonal variability of diurnal in-stream nitrate concentration  
556 oscillations under hydrologically stable conditions. *Biogeochemistry* 97:123–140.

557 Schlesinger, W. H. 2009. On the fate of anthropogenic nitrogen. *Proceedings of the National*  
558 *Academy of Sciences of the United States of America* 106:203–8.

559 Scholefield, D., T. Le Goff, J. Braven, L. Ebdon, T. Long, and M. Butler. 2005. Concerted  
560 diurnal patterns in riverine nutrient concentrations and physical conditions. *The Science of the*  
561 *Total Environment* 344:201–210.

562 Sudduth, E. B., S. S. Perakis, and E. S. Bernhardt. 2013. Nitrate in watersheds: Straight from  
563 soils to streams? *Journal of Geophysical Research: Biogeosciences* 118:291–302.

564 Sutton, M. A, O. Oenema, J. W. Erisman, A. Leip, H. van Grinsven, and W. Winiwarter. 2011.  
565 Too much of a good thing. *Nature* 472:159–61.

566 Sterner, R. W., and J. J. Elser. 2002. *Ecological stoichiometry: The biology of elements from*  
567 *molecules to the biosphere*. Princeton University Press, editors. Princeton, NJ.

568 Tank, J. L., E. J. Rosi-Marshall, M. A. Baker, and R. O. Hall, Jr. 2008. Are rivers just big  
569 streams? A pulse method to quantify nitrogen demand in a large river. *Ecology* 89:2935–2945.

570 Technicon. 1976. Technicon Instrument System. In Technicon, editors. *Technicon Method*  
571 *Guide*. Tarrytown, NY.

572 Valett, H. M., S. A. Thomas, P. J. Mulholland, J. R. Webster, C. N. Dahm, C. S. Fellows, C. L.  
573 Crenshaw, and C. G. Peterson. 2008. Endogenous and exogenous control of ecosystem function:  
574 N cycling in headwater streams. *Ecology* 89:3515–3527.

575 Volkmar, E. C., S. S. Henson, R. A. Dahlgren, A. T. O’Geen, and E. E. Van Nieuwenhuysen.  
576 2011. Diel patterns of algae and water quality constituents in the San Joaquin River, California,  
577 USA. *Chemical Geology* 283:56–67.

578 Young, R. G., and A. D. Huryn. 1998. Comment: Improvements to the diurnal upstream-  
579 downstream dissolved oxygen change technique for determining whole-stream metabolism in  
580 small streams. *Canadian Journal of Fisheries and Aquatic Sciences* 55:1784–1785.

581 Zar, J. H. 2010. *Biostatistical analysis in* Prentice-Hall/Pearson, editors. Upper Saddle River, NJ.

582 **Appendix A: Contribution of riparian groundwater inputs to day-night variations in**

583 **stream nitrate concentration**

584

585 **Tables**

586 *Table 1:* Mean daily stream water temperature (T), daily photosynthetically active radiation  
 587 ( $\Sigma$ PAR), hours per day with  $\text{PAR}_i > 200 \mu\text{mol m}^{-2} \text{s}^{-1}$  ( $\text{PAR}_{200}$ ), days with  $T > 10 \text{ }^\circ\text{C}$  ( $T_{10}$ ), and  
 588 days with  $\Sigma\text{PAR} > 4 \text{ mol m}^{-2} \text{d}^{-1}$  ( $\Sigma\text{PAR}_4$ ) for the up-, mid-, and down-stream sites during spring  
 589 2012. Values are medians and the 25<sup>th</sup> and 75<sup>th</sup> percentile are shown in brackets. For T,  $\Sigma$ PAR  
 590 and  $\text{PAR}_{200}$ , different letters indicate statistical significant differences between sampling sites  
 591 (Wilcoxon paired rank sum test, p-value < 0.05, df = 1; for the three variables n = 112).

592

| Site               | T<br>( $^\circ\text{C}$ )      | $\Sigma$ PAR<br>( $\text{mol m}^{-2}\text{d}^{-1}$ ) | $\text{PAR}_{200}$<br>(hours/day) | $T_{10}$<br>(days) | $\Sigma\text{PAR}_4$<br>(days) |
|--------------------|--------------------------------|--|-----------------------------------|--------------------|--------------------------------|
| <b>Up-stream</b>   | 10.2 [8.6, 13.2] <sup>A</sup>  | 4.1 [3.6, 4.8] <sup>A</sup>                          | 0.5 [0.0, 1.5] <sup>A</sup>       | 57                 | 66                             |
| <b>Mid-stream</b>  | 12.2 [10.4, 14.5] <sup>B</sup> | 5.2 [4.1, 6.1] <sup>B</sup>                          | 1.0 [0.5, 1.5] <sup>A</sup>       | 99                 | 83                             |
| <b>Down-stream</b> | 12.4 [10.4, 14.5] <sup>B</sup> | 8.9[6.3, 11.9] <sup>C</sup>                          | 2.5 [1.5, 4.0] <sup>B</sup>       | 103                | 104                            |

593

594



595 **Figure captions**

596 *Figure 1.* Map of the Font del Regàs catchment (Montseny Natural Park, NE Spain). The  
597 location of the three sampling sites along the stream continuum is shown with circles. The up-  
598 stream site was located 0.6 km upstream of the first tributary discharging to the mainstem. The  
599 mid- and down-stream sites were located 1.7 and 2.9 km downstream of the up-stream site,  
600 respectively. The piezometer located in the riparian area of the down-stream site is shown with a  
601 square.

602 *Figure 2.* Temporal pattern of (a) mean daily stream water temperature (T), (b) daily  
603 photosynthetically active radiation ( $\Sigma$ PAR) and (c) stream metabolism during spring 2012 at the  
604 down-stream site. In panel (a) and (b), different colors showed data for the up-stream (black),  
605 mid-stream (dark grey) and down-stream (grey) sampling site. Dashed lines indicate thresholds  
606 upon which photoautotrophs are not limited by temperature ( $T = 10^{\circ}\text{C}$ ) or light ( $\Sigma\text{PAR} = 4 \text{ mol}$   
607  $\text{m}^{-2} \text{d}^{-1}$ ). In panel (c), different colors showed data for GPP (black) and ER (grey).

608 *Figure 3.* Diel variation of (a) stream water temperature (Temp), (b) photosynthetically active  
609 radiation ( $\text{PAR}_i$ ), (c) stream discharge (Q), (d) stream  $\text{Cl}^-$  concentration, and (e) stream  $\text{NO}_3^-$   
610 concentration during spring 2012 at the down-stream site. Black arrows indicate the beginning  
611 and the end of the leaf emergence period (Poblador, unpublished data).

612 *Figure 4.* Temporal pattern of the relative difference between midnight and noon stream water  
613 concentrations ( $\Delta_{\text{solute}}$ ) for both chloride (white) and nitrate (black) at the (a) up-stream, (b) mid-  
614 stream, and (c) down-stream sites during the water-year 2010-2011. Circles are the median of

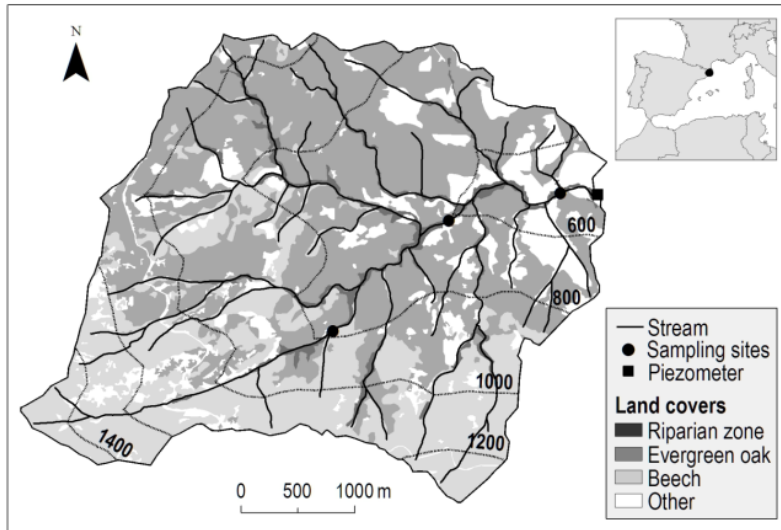
615  $\Delta_{\text{solute}}$  for each month and whiskers denote the 25<sup>th</sup> and 75<sup>th</sup> percentile. The black line indicates  
616 no differences between midnight and noon solute concentrations.

617 *Figure 5.* Temporal pattern of the relative difference between midnight and noon concentrations  
618 ( $\Delta_{\text{solute}}$ ) for both chloride (white) and nitrate (black) in (a) stream water, and (b) riparian  
619 groundwater during spring 2012 at the down-stream site. Circles are the median of  $\Delta_{\text{solute}}$  for  
620 each week and whiskers denote the 25<sup>th</sup> and 75<sup>th</sup> percentile. The black line indicates no  
621 differences between midnight and noon solute concentrations.

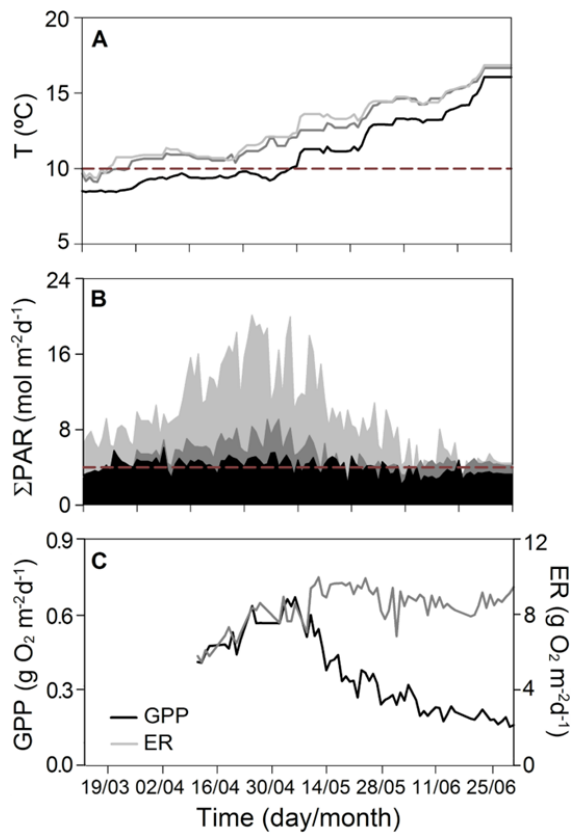
622 *Figure 6.* Relationship between (a) daily photosynthetically active radiation ( $\Sigma\text{PAR}$ ) and daily  
623 gross primary production (GPP), (b) daily GPP and day-night variations in stream nitrate  
624 concentration ( $\Delta_{\text{NO}_3}$ ), and (c) observed and stoichiometrically predicted day-night variations in  
625 stream nitrate concentration during spring 2012 at the down-stream site. The black line in panels  
626 (a) and (b) is the linear regression between variables (GPP vs.  $\Sigma\text{PAR}$ : l.r.,  $R^2 = 0.74$ ,  $p < 0.001$ ;  
627  $\Delta_{\text{NO}_3}$  vs. GPP: l.r.,  $R^2 = 0.74$ ,  $p < 0.001$ ). The 1:1 line is indicated in panel (c) with a dashed line.  
628 White circles in panel (c) indicated day-night variations in stream nitrate concentration in June.

629 **Figures**

630 *Figure 1*

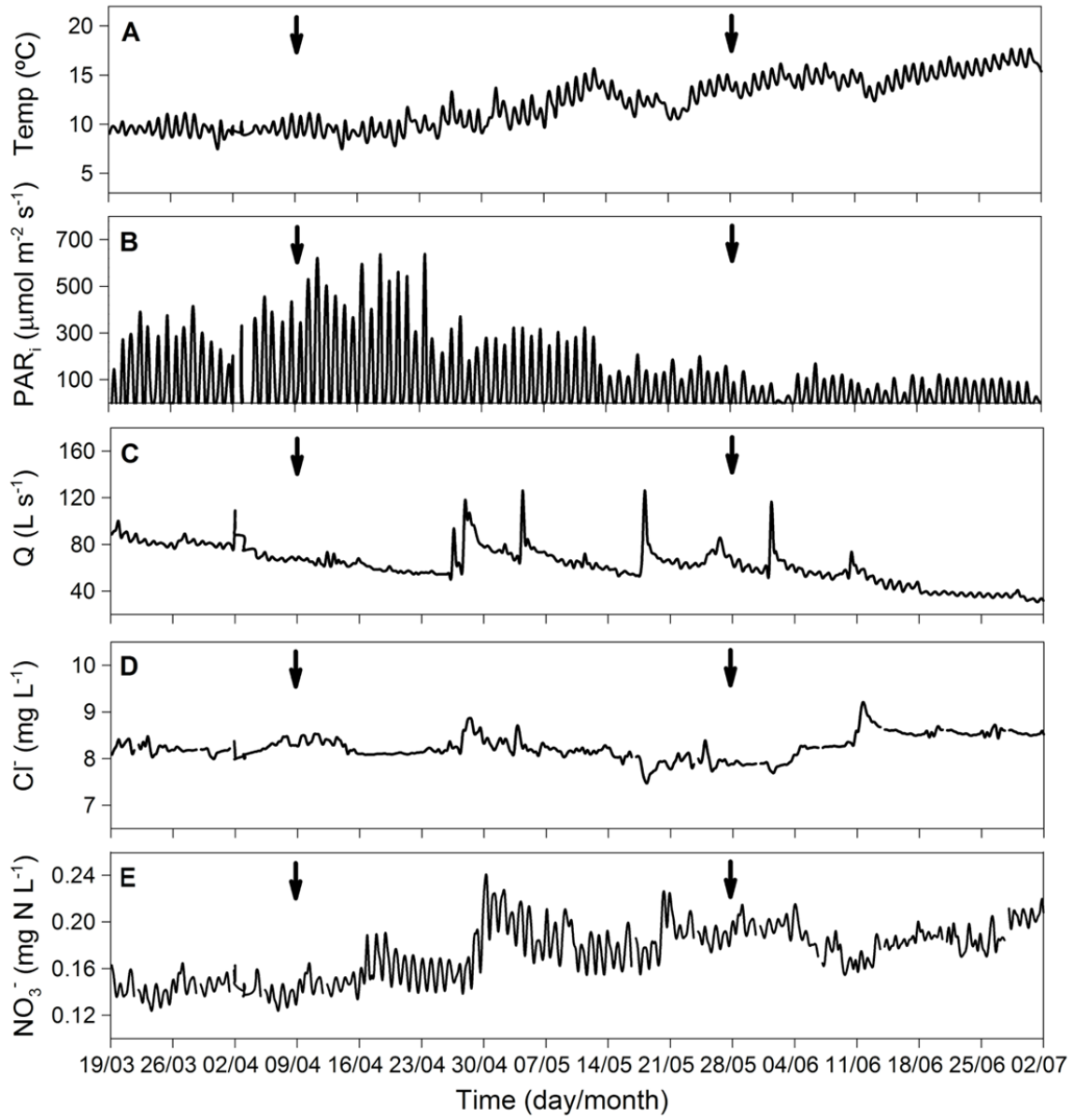


631



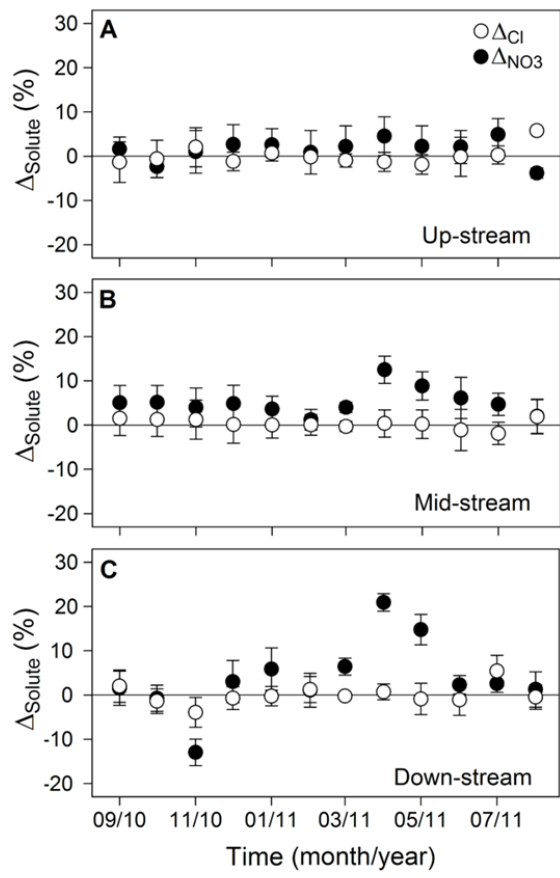
634

635 *Figure 3*



636

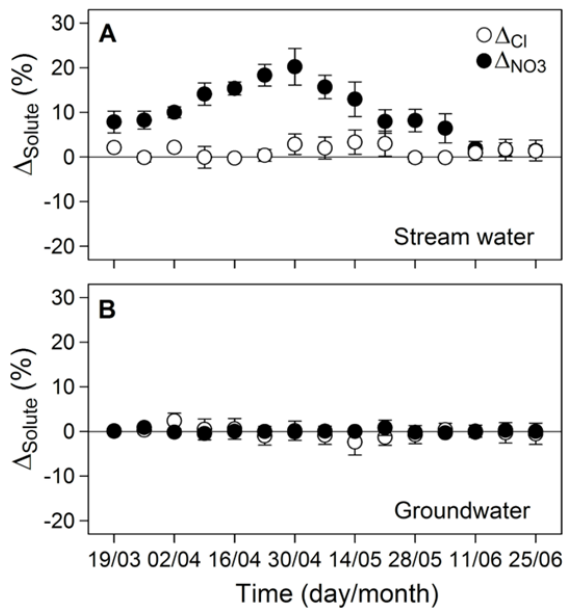
637 *Figure 4*



638

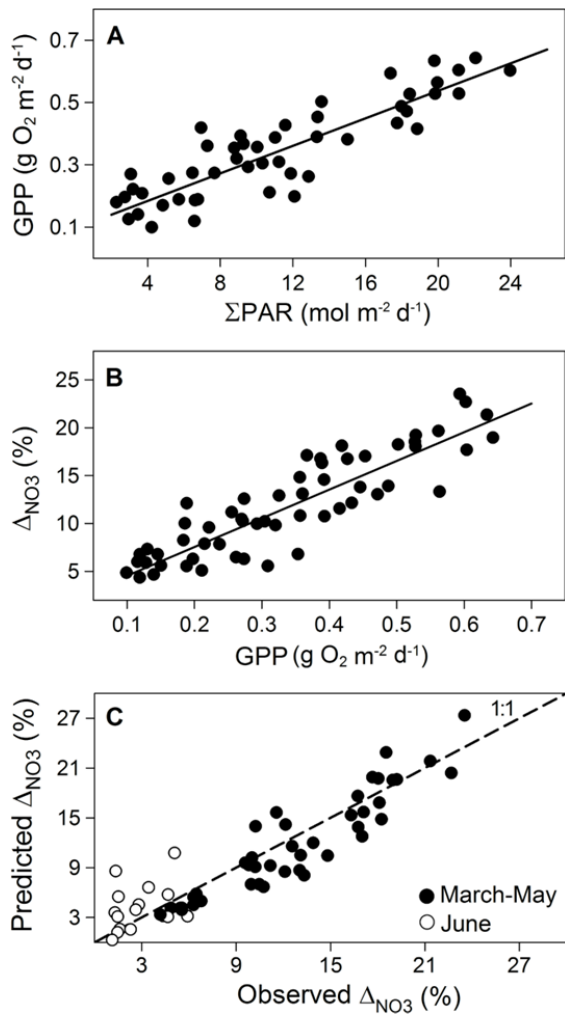
639

640 *Figure 5*



641

642 *Figure 6*



643

644





1 **Title: Green light: gross primary production influences seasonal stream N export by**  
2 **controlling fine-scale N dynamics**

3 **Authors**

4 *Anna Lupon<sup>1</sup>, Eugènia Martí<sup>2</sup>, Francesc Sabater<sup>1</sup> Susana Bernal<sup>1,2</sup>*

5 **Appendix A**

6 **Title: Contribution of riparian groundwater inputs to day-night variations in stream**  
7 **nitrate concentration**

8 We considered the possibility that day-night fluctuations in riparian groundwater inputs suffice  
9 to explain the observed diel variations in stream nitrate ( $\text{NO}_3^-$ ) concentration during spring 2012  
10 at the down-stream site. We used a mass balance approach to calculate midnight  $\text{NO}_3^-$   
11 concentrations based solely on hydrological mixing. For each day:

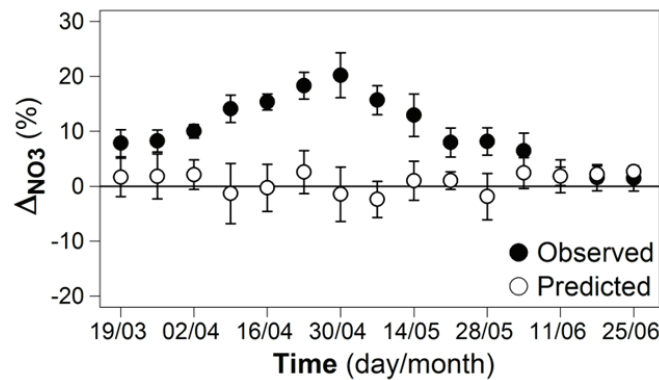
$$12 \quad [\text{NO}_3^-]_{\text{sw}(0\text{h})} = \frac{[\text{NO}_3^-]_{\text{sw}(12\text{h})} * Q_{\text{sw}(12\text{h})} + [\text{NO}_3^-]_{\text{gw}} * Q_{\text{sw}(0\text{h}-12\text{h})}}{Q_{\text{sw}(0\text{h})}}, \quad (\text{A.1})$$

13 where  $[\text{NO}_3^-]_{\text{sw}}$  is stream  $\text{NO}_3^-$  concentration and  $[\text{NO}_3^-]_{\text{gw}}$  is the average of riparian groundwater  
14  $\text{NO}_3^-$  concentration between midnight and noon (all in  $\text{mg N L}^{-1}$ ).  $Q_{\text{sw}}$  is stream discharge and  
15  $Q_{\text{sw}(0\text{h}-12\text{h})}$  is riparian groundwater input estimated as the difference in  $Q_{\text{sw}}$  between midnight and  
16 noon (all in  $\text{L s}^{-1}$ ). The subscripts (0h) and (12h) denote time of the day, midnight and noon  
17 respectively. We calculated the relative difference between midnight  $\text{NO}_3^-$  concentrations  
18 predicted from hydrological mixing and those observed at noon ( $\Delta_{\text{NO}_3}$ , in %) (Eq. 1, main  
19 manuscript). Moreover, we used a Wilcoxon paired rank sum test to examine whether

20 differences between  $\text{NO}_3^-$  concentrations observed at noon and those predicted for midnight were  
21 statistically significant (Zar 2010).

22 During spring 2012, midnight stream  $\text{NO}_3^-$  concentration predicted from hydrological mixing  
23 were similar to those observed at noon (for each week from March to June:  $Z > Z_{0.05}$ ,  $df = 6$ ,  $p >$   
24  $0.1$ ). The average  $\Delta_{\text{NO}_3}$  calculated from predicted midnight  $\text{NO}_3^-$  concentrations was 0.6%  
25 (Figure A1, white circles). This value was 20 fold lower than the  $\Delta_{\text{NO}_3}$  obtained from observed  
26 midnight and noon  $\text{NO}_3^-$  concentrations (13%) (Figure A1, black circles). Similar results were  
27 obtained when using midnight rather than average riparian groundwater  $\text{NO}_3^-$  concentration.  
28 These findings, together with the fact that no simultaneous diel variations in discharge, riparian  
29 groundwater level and N concentrations were observed, support the idea that terrestrial processes  
30 did not control diel variations in  $\text{NO}_3^-$  concentrations at the study site.

### 31 Figures



32  
33 *Figure A1.* Temporal pattern of the relative difference between midnight and noon stream nitrate  
34 concentrations ( $\Delta_{\text{NO}_3}$ ) during spring 2012 at the down-stream site. The  $\Delta_{\text{NO}_3}$  is shown for  
35 observed values and for values predicted from hydrological mixing (black and white circles,

36 respectively). Symbols are the median of  $\Delta_{\text{NO}_3}$  for each week and whiskers denote the 25<sup>th</sup> and  
37 75<sup>th</sup> percentiles. The black line indicates no differences between midnight and noon nitrate  
38 concentrations.

### 39 **Refernces**

40 Zar, J. H. 2010. *Biostatistical analysis in* Prentice-Hall/Pearson, *editors*. Upper Saddle River, NJ.